World Academy of Science, Engineering and Technology
International Journal of Mechanical and Mechatronics Engineering
Vol:4, No:1, 2010

Theoretical Modeling and Experimental Study of Combustion and Performance Characteristics of Biodiesel in Turbocharged Low Heat Rejection D.I Diesel Engine

B.Rajendra Prasath, P.Tamilporai, and Mohd.F.Shabir

Abstract**—**An effort has been taken to simulate the combustion and performance characteristics of biodiesel fuel in direct injection (D.I) low heat rejection (LHR) diesel engine. Comprehensive analyses on combustion characteristics such as cylinder pressure, peak cylinder pressure, heat release and performance characteristics such as specific fuel consumption and brake thermal efficiency are carried out. Compression ignition (C.I) engine cycle simulation was developed and modified in to LHR engine for both diesel and biodiesel fuel. On the basis of first law of thermodynamics the properties at each degree crank angle was calculated. Preparation and reaction rate model was used to calculate the instantaneous heat release rate. A gas-wall heat transfer calculations are based on the ANNAND's combined heat transfer model with instantaneous wall temperature to analyze the effect of coating on heat transfer. The simulated results are validated by conducting the experiments on the test engine under identical operating condition on a turbocharged D.I diesel engine. In this analysis 20% of biodiesel (derived from Jatropha oil) blended with diesel and used in both conventional and LHR engine. The simulated combustion and performance characteristics results are found satisfactory with the experimental value.

Keywords**—**Biodiesel, Direct injection, Low heat rejection, Turbocharged engine

I. INTRODUCTION

DIESEL engines are broadly used in medium and heavy-duty applications because of their lower fuel consumption, higher brake thermal efficiency and lower emissions (such as CO and HC) compared with gasoline engines. Depletion of petroleum derivatives increases the research interest in the area of alternative fuels. The high viscosity and low volatility of raw vegetable oils are generally considered to be the major drawbacks for their utilization as fuels in diesel engines. The usage of raw vegetable oils in diesel engines leads to injector coking, severe engine deposits, filter gumming problems, piston ring sticking and thickening of the lubricating oil [1]–[8]. However, these effects can be reduced through the esterification of the vegetable oil to form monoesters called as biodiesel [9], [10]. Biodiesel produced [11]-[15] from the non- edible Jatropha oil decreases viscosity and improves the cetane number and heating value.

Thermal barrier coatings are used to improve the engine performance and efficiency of internal combustion engines [16]-[21]. The engine with thermal barrier coating is called low heat rejection (LHR) engine, which is based on suppressing the heat rejection to the coolant and recovering the energy. The engines parts such as piston, cylinder head, cylinder liners and valves are coated with partially stabilized zirconia (PSZ)[22], [23]. The superior advantages of LHR engines are improved fuel economy, higher energy in exhaust gases and capability of handling higher viscous fuel. The transesterification process brings down the properties of fuel closer to the diesel fuel. The higher temperature of the LHR engine increases the possibility of using biodiesel without preheating.

The development of computer technology narrows down the time consumption for the sophisticated engine test through the simulation techniques. The insight of the combustion process is to be analyzed thoroughly, which enhance the power out put of the engine and consider as the heart of the engine process [24], [25]. Thermodynamic models are mainly based on the first law of thermodynamics and are used to analyze the combustion and performance characteristics of engines. A computer code was developed using "C" language for conventional engine and converted in to LHR engine application through the wall heat transfer model [26].

II.TRANSESTERIFICATION OF VEGETABLE OIL

The vegetable oil was transesterified using methanol in the presence of NaOH as a catalyst. The parameter involved in the processing such as catalyst amount, molar ratio of alcohol to oil, reaction temperature and reaction time are optimized [27], [28]. The fundamental Transesterification chemistry and

B.Rajendra Prasath is with the Tagore Engineering College, Department of Mechanical Engineering, Anna University, Chennai, India (Phone:+91-4427409725, fax:+91-4427409729, e-mail:br_prasath@rediffmail.com).

P.Tamilporai is with the College of Engineering, Guindy, Department of Mechanical Engineering, Internal Combustion Engineering Division, Anna University, Chennai, India (e-mail: tporai@annauniv.edu).

Mohd.F.Shabir is with the Tagore Engineering College, Department of Mechanical Engineering, Anna University, Chennai, India (e-mail: ffshabir2001@yahoo.co.in).

trasesterification process are shown in Fig.1 and Fig.2 respectively.

$$\begin{array}{lcccl} CH_2OOCR & & & & CH_2OH \\ CHOOCR & +3CH_3OH & \rightarrow & 3CH_3OOCR + & CHOH \\ CH_2OOCR & & & & CH_2OH \\ \text{Triglycerides} & \text{Methanol} & & \text{Methyl Ester} & \text{Glycerol} \end{array}$$

Fig. 1 Transesterification chemistry

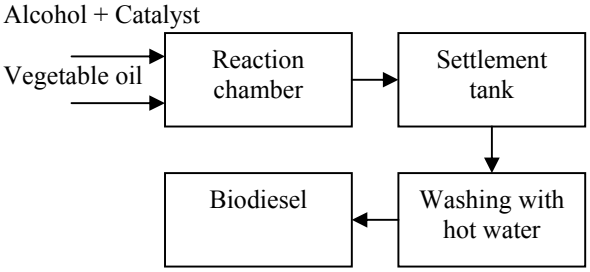

Fig. 2 Transesterification process

Known quantity of vegetable oil was taken in a three-necked round-bottomed flask. A water-cooled condenser and a thermometer with cork were connected to the side openings on either side of the round-bottomed flask. The required amount of catalyst (NaOH) was weighed and dissolved completely in the required amount of methanol by using a stirrer to form sodium methoxide solution in the case of base/alkali catalyst. Meanwhile, the oil was warmed by placing the round-bottomed flask in the water bath maintained at the selected temperature mentioned above. The sodium methoxide solution was added into the oil for vigorous mixing by means of a mechanical stirrer fixed into the flask. The required temperature was maintained throughout the reaction time and the reacted mixture was poured into the separating funnel. The mixture was allowed to separate and settled down by gravity settling into a clear, golden liquid biodiesel on the top with the light brown glycerol at the bottom. The glycerol was drained off from the separating funnel leaving the biodiesel/ester at the top. The raw biodiesel was collected and water washed to bring down the pH of biodiesel to 7. This pure biodiesel gives the ester yield measured on weight basis and the important fuel and chemical properties were determined.

III. PREPARATION OF TEST FUEL

In this experimental study diesel and biodiesel was used as a fuel for standard (STD) engine and low heat rejection (LHR) engine. 20% by volume of biodiesel was taken in a cleaned vessel, which is mixed with 80% by volume of diesel, and thus a stable mixture (hereafter the biodiesel blend is simply referred as biodiesel) was prepared to use in the test engine.

TABLE I PROPERTIES OF FUELS

Properties	Diesel	B100	B20
Density @ 15°C(kg/m^3)	830	880	840
Viscosity @ 40°C(cSt)	2.8	4.6	3.15
Flash point (°C)	55	170	80
Cetane number	45	50	46
Lower Heating Value (MJ/kg)	42	36	40.5

IV. TEST ENGINE AND EXPERIMENTAL PROCEDURE

The experiment was conducted on the four cylinder four stroke turbocharged water cooled engine with the specifications shown in Table 2.

Loading

The engine test bed consists of a test engine, hydraulic dynamometer, measurement instruments and control panel. The hydraulic dynamometer is water cooled and rated for 112 kW power absorption at 3000 rpm maximum operating speed. The load on the dynamometer was measured by using a mechanical dial gauge that was calibrated by using standard weights just before the experiments.

TABLE II SPECIFICATION OF THE TEST ENGINE

Bore, mm	111
Stoke length, mm	127
Connecting rod length, mm	251
Compression ratio	16:1
Displacement volume, liter	4.9134
Maximum power, HP	75
Injection pressure, bar	200
Inlet valve open (IVO)	8° BTDC
Inlet valve closing (IVC)	45° ABDC
Exhaust valve open (EVO)	45° BBDC
Exhaust valve closing (EVC)	12° ATDC
Injection timings, degrees	26° BTDC

Temperatures measurement

Exhaust gas temperature after the turbine and after the compressor (before inlet valve) was measured using iron-constantan thermocouple. The input signal was given to the 8 channel digital indicator. A mercury-in-glass thermometer was used to measure the cooling water temperature

.

Pressure measurement

A piezoelectric transducer was installed in the engine cylinder head in order to measure the combustion pressure. Signal from the pressure transducer were fed to charge amplifier. A magnetic shaft encoder was used to give the signal for TDC position against crank angle. The signals from the charge amplifier and shaft encoder were coupled to data acquisition system.

Fuel flow measurement

Fuel consumption was measured using fuel flow meter by noting the time taken for 20 cc fuel consumption.

Air flow measurement

Mass of air requirement for different speed was measured using air box method fitted with simple U tube water manometer by noting head difference.

Both the diesel and biodiesel (20% biodiesel and 80% diesel)fuels are used in the STD engine and LHR engine with different speeds such as 1000, 1100, 1200, 1300, 1400, 1500 rpm. The simulation and experimental studies were made for the following four combinations.

1. Turbocharged conventional engine operated with diesel (denoted by STD Diesel)
2. Turbocharged conventional engine operated with biodiesel (denoted by STD Biodiesel)
3. Turbocharged LHR engine operated with diesel (denoted by LHR Diesel)
4. Turbocharged LHR engine operated with biodiesel (denoted by LHR Biodiesel)

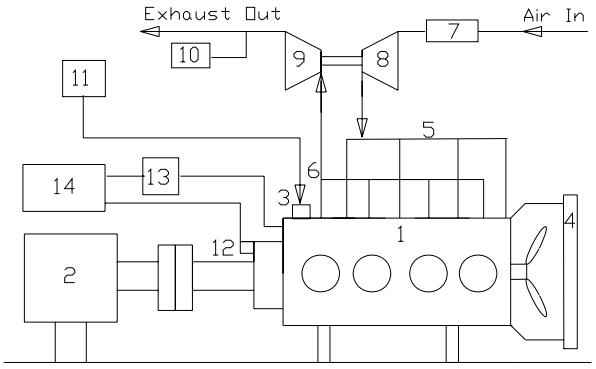

Fig. 3 Schematic of experimental set up

1. Test Engine
2. Hydraulic dynamometer
3. Fuel pump
4. Radiator
5. Intake manifold
6. Exhaust manifold
7. Air box
8. Compressor handling intake air
9. Turbine handling exhaust gas
10. Exhaust gas analyzer
11. Fuel tank
12. Crank angle encoder
13. Charge amplifier
14. Computer with CRO

The tests were performed at full load condition for the engine speeds from 1000 to 1500 rpm with 100 rpm step. The ambient, cooling water and exhaust gas temperatures before the turbine inlet were measured by K type thermocouples. The thermocouples were connected to a multi-channel temperature indicator. Fuel consumption was measured with a constant volume burette with stopwatch. Air flow rate was measured through air box connected with water manometer. First, diesel fuel was used as fuel and then biodiesel was used as fuel. After completion of the test of standard (STD) engine, the cylinder head and valves were coated with plasma sprayed Partially Stabilized Zirconia (PSZ) of 0.5 mm thickness, as the test engine was converted to a LHR condition. The same test procedure was conducted for the LHR engine and the experimental results were compared with simulation results.

V.CONVERSION OF STANDARD ENGINE (STD) IN TO LOW HEAT REJECTION (LHR) ENGINE

Increasing the coating thickness decreases the volumetric efficiency and hence work done. In this experimental study ceramic coating thickness was optimized as 0.5 mm [22], [23]. The engine combustion chamber was coated with partially stabilized zirconia (PSZ) of 0.5 mm thickness, which includes the piston crown, cylinder head, valves, and outside of the cylinder liner. The equal amount of material has been removed from the various parts of the combustion chamber and PSZ was coated uniformly. After PSZ coating, the engine was allowed to run about 10 hours, then test were conducted on it.

The present work involves to usage of biodiesel in LHR engine to analyze the combustion and performance characteristics. To validate the theoretical results, experiments were conducted on a turbocharged direct injection (DI) diesel engine and LHR engine using diesel and biodiesel under identical operating condition.

VI. THEORETICAL MODELING

The formula and empirical relations used for diesel cycle simulation are considered and are explained in the following chapter. In this analysis the molecular formula for diesel and bio diesel are approximated, as $C_{10}H_{22}$ and $C_{19}H_{34}O_2$ [29]. The combustion model is developed for the C.I engine and suitable for any hydrocarbon fuel and their blends. The molecular formula of fuel is given as one of the input to the model along with the other inputs shown in table.

Number of Moles of Reactants and Products

In this simulation during the start of combustion, the moles of different species are considered includes O_2 , N_2 from intake air and CO_2, H_2O, N_2 and O_2 from the residual gases. The overall combustion equation considered for the fuel with C-H-O-N is

Fundamental combustion equation

$$C_xH_yO_z + \lambda * y_{cc} * (O_2 + 3.773N_2) \longrightarrow$$

$$xCO_2 + (y/2)H_2O + (\lambda - 1)y_{cc}O_2 + \lambda y_{cc} * 3.773N_2 \quad (1)$$

x - No. of moles of carbon
y - No. of moles of hydrogen
z - No. of moles of oxygen
Stochiometric AFR $y_{cc} = x + (y/4) - (z/2)$
λ - Excess air factor

Calculation of Total Moles of Reactants and Products

Total number of reactants and products during the start of combustion as well every degree crank angle was calculated from the equations.

$$tmr = 1 + \lambda * y_{cc} * 4.773 \quad (2)$$

$$tmp = x + (y/4) + 3.773 * \lambda * y_{cc} + (\lambda - 1) * y_{cc} \quad (3)$$

tmr - total moles of reactants
tmp - total moles of products

Volume at any Crank Angle

Volume at any crank angle is calculated from this equation

$$V_\theta = V_C + \left(\pi * \frac{d^2}{4} * \frac{l}{2}\right) * \left(1 + Z - \left(Z^2 - \sin^2\theta\right)^{\frac{1}{2}} - \cos\theta\right) \quad (4)$$

$$Z = 2 * (L/l)$$

d - Cylinder diameter, m
L - Connecting rod length, m
l - Stroke length, m
V_θ - Volume at any crank angle, m^3
V_c - Clearance volume, m^3
θ - Crank angle, degrees

Calculation of Specific Heat

Specific heat at constant volume for each species is calculated using the expression given below

$$Cv(T) = (B - \bar{R}) + \frac{C}{T} \quad (5)$$

Total specific heat of all species is

$$Cp(T) = B + \frac{C}{T} \quad (6)$$

A, B and C are the coefficients of the polynomial equation

Initial Temperature and Pressure during Start of Compression

Initial temperature at the beginning of the compression process is calculated as follows

$$P_2 = \left(\frac{V_1}{V_2}\right) * \left(\frac{T_2}{T_1}\right) * P_1 \quad \text{and} \quad (7)$$

$$T_2 = T_1 * \left(\frac{V_1}{V_2}\right)^{\frac{R}{Cv(T_1)}} \quad (8)$$

T_1- Initial temperature, K
T_2- Final temperature, K
P1 - Initial pressure, bar
P2 - Final pressure, bar
R - Charecteristic gas constant, kJ/kgK
C_v- Specific heat at constant volume,kJ/kgK

Enthalpy

Enthalpy of each species is calculated from the expression given below which is used to calculate the peak flame temperature of the cyclic process.

$$H(T) = A + B*T + C*\ln(T) \quad (9)$$

Internal Energy

The internal energy for each species and overall internal energy are calculated from the expressions given below

$$U(T) = A + (B - \bar{R}) * T + C * \ln(T) \text{ and} \quad (10)$$

$$U(T) = \sum (x_i U_i(T)) \quad (11)$$

A, B and C are the coefficients of the polynomial equation.

Work Done

Work done in each crank angle is calculated from

$$dW = \left(\frac{P_1 + P_2}{2}\right)(V_2 - V_1) \quad (12)$$

V_1 - Initial volume, m^3
V_2 - Final volume, m^3

Total Heat Transfer

The gas-wall heat transfer is found out using ANNAND'S convective heat transfer model. Radiation heat transfer was also estimated using this model. A wall heat transfer model is used to find out the instantaneous wall temperature. First term of this equation shows that Prandtl number for the gases forming the cylinder contents will be approximately constant at a value 0.7, claims that Reynolds number is the major parameter affecting convection. The second is a straightforward radiation term assuming gray body radiation.

$$\frac{dQ}{dt} = ak\frac{\mathrm{Re}^b}{d}(T_g - T_W) + c(T_g^4 - T_W^4) \quad (13)$$

dQ/dt - Heat transfer rate, kJ/CA
T_g - Gas temperature, K
T_w - Wall temperature, K
Re - Reynolds number
a, b and c are the constants of the equations
Viscosity of air at each temperature change is calculated from

$$\mu_{air} = 3.3 * 10^{-7} (T)^{0.7} \quad (14)$$

Viscosity of the combustion gases are calculated from

$$\mu_{prod} = \frac{\mu_{air}}{(1 + 0.027\phi)} \quad (15)$$

Φ - Equivalence ratio
Reynolds number for each time step is calculated as the viscosity varies

$$\mathrm{Re} = \frac{\rho d V_p}{\mu_{prod}} \quad (16)$$

ρ - Density of gas mixture, kg/m^3
V_p - Mean piston speed, m/min
Thermal conductivity is calculated for each change in viscosity

$$k = \frac{C_p \mu_{prod}}{0.7} \quad (17)$$

Heat transfer coefficient

Heat transfer coefficient of gases for each degree crank angle is calculated from the following equation.

$$h_g = 0.26 * (k/d) * R_e^{0.6} \quad (18)$$

Wall Heat Transfer Model

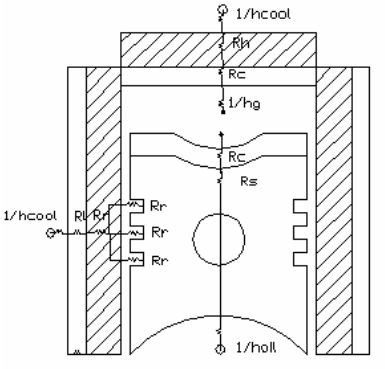

Fig. 4 Thermal network model for wall heat transfer

Thermal network model was developed (for wall heat transfer analysis) are used to analyze the effect of coating on engine heat transfer. The model used to analyze the heat transfer through cylinder to the coolant and thereby to find instantaneous wall temperature. Initial temperature is found out using the following expression

$$T_w = T_g - \left(Q_w / 2\pi h_g r l\right) \tag{19}$$

T_w - Wall temperature, K
h_g - heat transfer coefficient of gas, w/m^{2}K

The total resistance(R_t) offered by the cylinder liner, piston rings, cylinder head, ceramic coating and piston for the heat transfer from cylinder gases to coolant is given by the following equation.

$$R_t = (1/2\pi h_g r_1 l) + \log_e(r_2/r_1)/(2\pi k_1 l_1)$$
$$\log_e(r_3/r_4)/(2\pi k_c l_c) + 3\log_e(r_5/r_9)/(2\pi k_r l_r)$$
$$\log_e(r_7/r_8)/(2\pi k_s l_s) + (r_7/2\pi r_7 k_p t_p) \tag{20}$$

Energy Equation
According to first law of thermodynamics the energy balance equation is given by

$$E(T_2) = E(T_1) - dW - dQ + dM_f Q_{VS} \tag{21}$$

To find the correct value of T2, both sides of the above equation should be balanced. So the above equation is rearranged as shown below

$$ER = E(T_2) - E(T_1) - dW - dQ + dM_f Q_{VS} \tag{22}$$

If the numerical value of ER is less than the accuracy required, then the correct value of T_2 has been established, otherwise a new value of T is calculated for new internal energy and C_V values.

$$ER' = C_V(T_2) * tmp \tag{23}$$

Newton-Rapshon techique

$$(T_2)_n = (T_2)_{n-1} - \frac{ER}{ER'} \tag{24}$$

Mass of Fuel Injected
Considering that nozzle open area is constant during the injection period, mass of the fuel injected for each crank angle is calculated using the following expression

$$M_f = C_d A_n \sqrt{2\rho_f \Delta P}\left(\frac{\Delta\theta_f}{360N}\right) \tag{25}$$

C_d- Coefficient of discharge of injector nozzle
A_n - cross sectional area of nozzle, m2
ΔP - Pressure drop across the nozzle, bar
N - Engine speed, rpm
$\Delta\theta_f$ - Fuel injection period, degrees

Unburned Zone Temperature

$$T_u = T_{SOC}\left(\frac{p}{p_{SOC}}\right)^{\frac{\gamma-1}{\gamma}} \tag{26}$$

T_u- Unburned zone temperature, K
T_{soc} - Temperature at the start of combustion, K
P_{soc} - Pressure at the start of combustion, bar
γ - Specific heat ratio

Preparation Rate
The preparation rate is calculated using the following equation given by

$$P_r = K M_f^{(1-x)} M_u^{\,x} P_{O2}^{\,L} \tag{27}$$
$$K = 0.085 N^{0.414} M_f^{1.414} \Delta\theta_f^{-1.414} n^{-1.414} d_n^{-3.644} \tag{28}$$

M_u - Mass of fuel unprepared, g/CA
n - No. of nozzle holes
d_n - Diameter of nozzle, m
x & L - Constant of equation
P_{O2} - Partial pressure of oxygen, bar

Reaction Rate
The reaction rate is calculated using the following equation

$$R_r = \frac{K' P_{O2}}{N\sqrt{T}} e^{\frac{-act}{T}} \int (P_r - R_r) d\theta \tag{29}$$

K' - Constant of equation
act - activation energy, kJ/kmol K

Initial Temperature during the start of combustion
Initial temperature during the start of combustion after the ignition delay is calculated using the equation given below

$$T_2 = T_1 + \frac{x_f Q_s}{C_v(T_1)} \tag{30}$$

x_f - Mass fraction of fuel burnt
Q_s- Total heat supply, kJ/kg

VII. RESULTS AND DISCUSSIONS

In this study combustion parameters like cylinder pressure, peak cylinder pressure and heat release are discussed. Performance parameters like brake thermal efficiency and specific fuel consumption are discussed. The results are compared with respect to LHR Biodiesel operation.

Cylinder pressure

In a CI engine the cylinder pressure is depends upon the fuel-burning rate during the premixed burning phase. The high cylinder pressure ensures the better combustion and heat release. The Fig.5 –Fig.8 shows the typical pressure variation with respect to crank angle. The advantages of higher temperature of LHR engine increases the cylinder pressure throughout the speed range. The cylinder pressure for LHR biodiesel is lower than LHR diesel about 1% and higher about 3.5%-5% and 3%-4.2% for STD biodiesel and STD diesel throughout the speed.

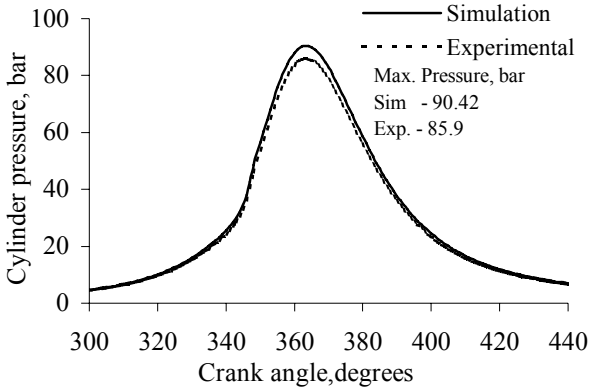

Fig. 5 Cylinder pressure with crank angle for STD Diesel at full load

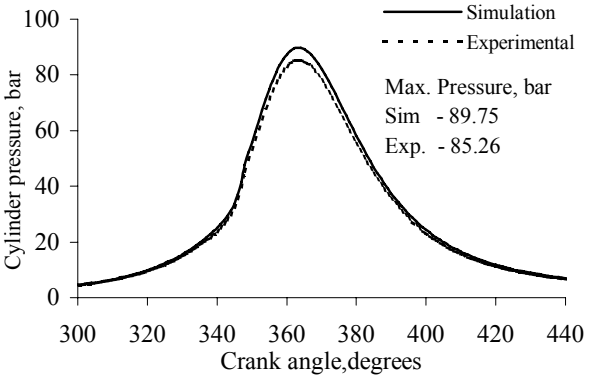

Fig. 6 Cylinder pressure with crank angle for STD Biodiesel at full load

Though the lower calorific value of biodiesel and higher initial temperature due to the domination of residual gases decreases the volumetric efficiency in LHR engine, thus reduces the peak pressure and work done. However the cylinder pressure for STD biodiesel is higher than STD diesel due to the oxygenated nature of biodiesel improves the combustion process.

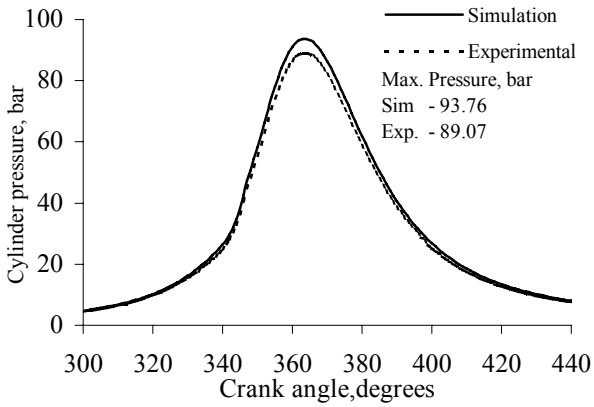

Fig. 7 Cylinder pressure with crank angle for LHR Diesel at full load

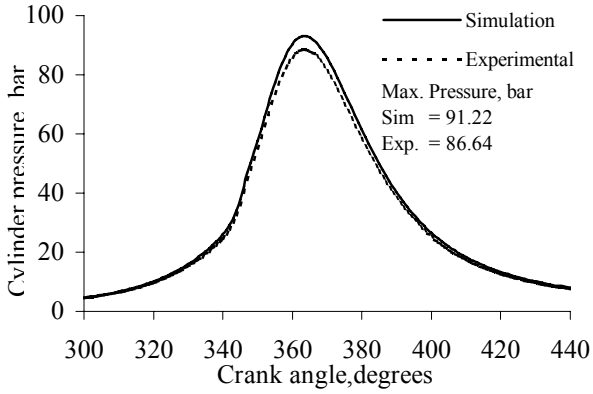

Fig. 8 Cylinder pressure with crank angle for LHR Biodiesel at full load

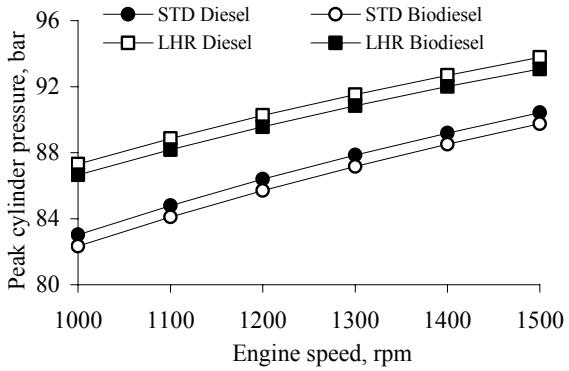

Fig. 9 Peak cylinder pressure at full load

It is noted that the maximum pressure obtained for biodiesel closer with TDC than diesel fuel. The fuel-burning rate in the early stage of combustion is more than the diesel fuel, which bring the peak pressure more close to TDC. During the expansion, the torque produced by the engine is kind enough to go for the next cycle with the consumption of more fuel.

The peak pressure of the engine is lower when using biodiesel then that of diesel. It may be due to lower quantity

of hydrocarbon in the biodiesel and lower pressure rise while burning. The oxygen atoms in the biodiesel molecule itself make the complete combustion of fuel and hence more energy is released. So that, biodiesel-fueled engine produces high peak temperatures than that of diesel-fueled engine. Peak pressure increases proportionately with engine speed as shown in Fig.9.

Cylinder Temperature

High pressure of compressed mixture increases its burning rate. This increases the peak pressure inside the combustion chamber. The comparisons of peak temperatures inside the cylinder for various combinations are shown in Fig10- Fig.13.

The presence of oxygen in the biodiesel makes complete combustion of fuel thereby producing more CO2 is produced and hence more heat is released from the gases. Thus, the peak temperature of biodiesel-fueled engine is higher than that of diesel fueled engine.

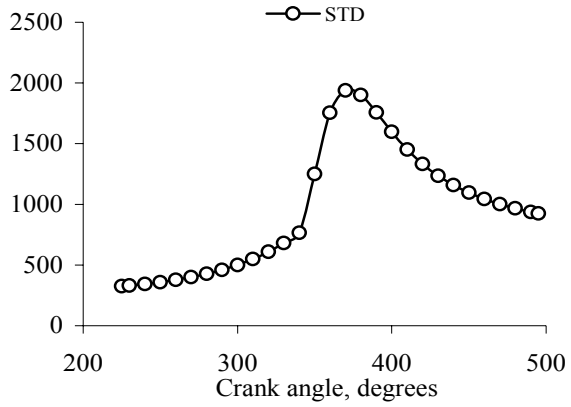

Fig. 10 Cylinder temperature with crank angle for STD Diesel at full load

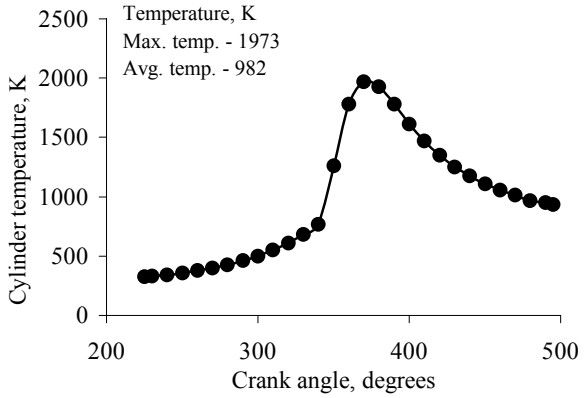

Fig. 11 Cylinder temperature with crank angle for STD Biodiesel at full load

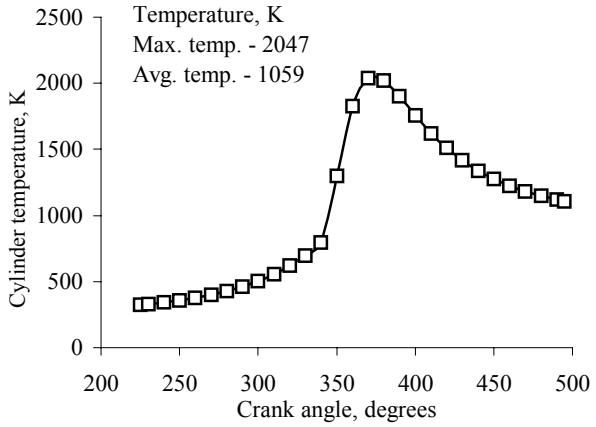

Fig. 12 Cylinder temperature with crank angle for LHR Diesel at full load

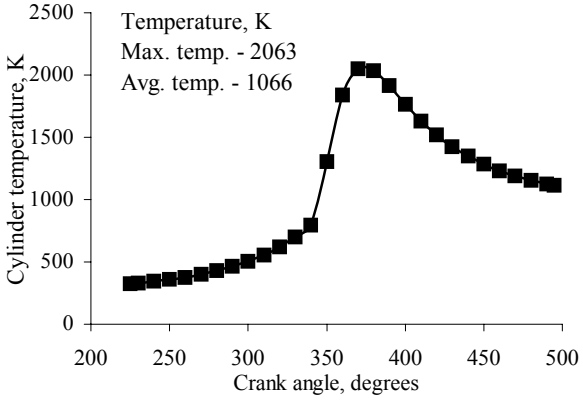

Fig. 13 Cylinder temperature with crank angle for LHR Biodiesel at full load

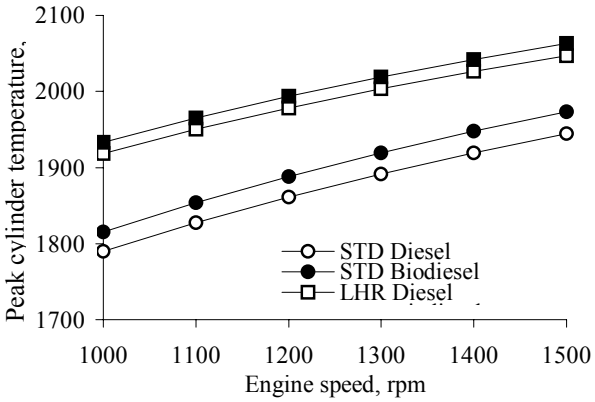

Fig.14 Peak cylinder temperature with engine speed at full load

The Fig.14 shows the typical variation of temperature with respect to engine speed. The peak cylinder temperature for LHR biodiesel is higher than LHR diesel STD biodiesel and STD diesel about 1%, 4.4%-6.1% and 5.8%-7.4% respectively from higher speed to lower speed.

Heat Release Rate

Fig.15 – Fig.18 shows the variation of heat release rate with crank angle. Both fuel experiences that the rapid premixed combustion followed by diffusion combustion. The premixed fuel burns rapidly and releases the enormous amount heat followed by the controlled heat release. The heat release rate during the premixed combustion is responsible for the high peak pressure. C.I engine combustion is divided in to four stages such as ignition delay, uncontrolled combustion, controlled combustion and after burning.

Ignition delay: The higher operating temperature reduces the ignition delay for both the fuel. However oxygenated nature of biodiesel further reduces the ignition delay. Combustion starts well in advance for LHR operation due to higher surrounding temperature.

Premixed combustion: Fuel droplets accumulated during the ignition delay period is responsible for the sudden heat release during this period is called premixed or uncontrolled combustion. Due to higher ignition delay of STD operation lower the heat release and higher the heat release for LHR operation during this period. The peak heat release for LHR was advanced few degree crank angle than STD operation due to shorter ignition delay and higher combustion temperature.

Diffusion combustion: After the evaporation of fuel droplets during the delay period, the fuel jets coming from the nozzle are converted in to fuel vapor is called diffusion combustion or controlled combustion. During this period both fuel in STD and LHR operation experience the smooth combustion and follow the similar pattern. However a marginal improvement was noticed for biodiesel.

After burning: The higher boiling point fuel molecules release the heat during this period called after burning. Higher the exhaust temperature for biodiesel fuel due to the complex structure of biodiesel and higher viscosity, hence higher exhaust temperature was noticed.

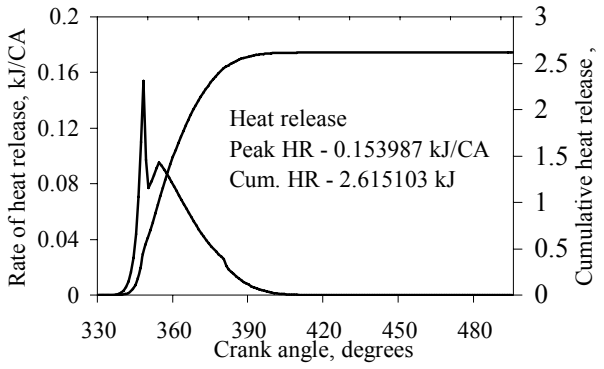

Fig. 15 Variation of heat release rate and cumulative heat release with crank angle for STD Diesel at full load

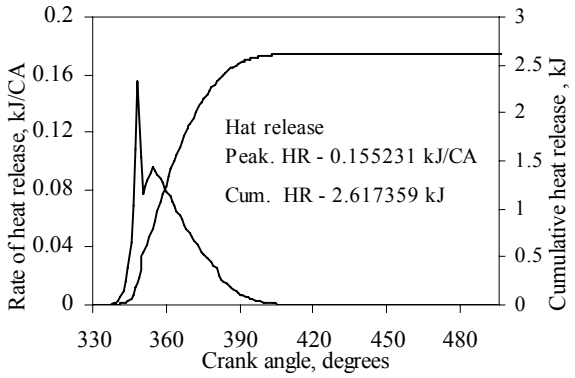

Fig. 16 Variation of heat release rate and cumulative heat release with crank angle for STD Biodiesel at full load

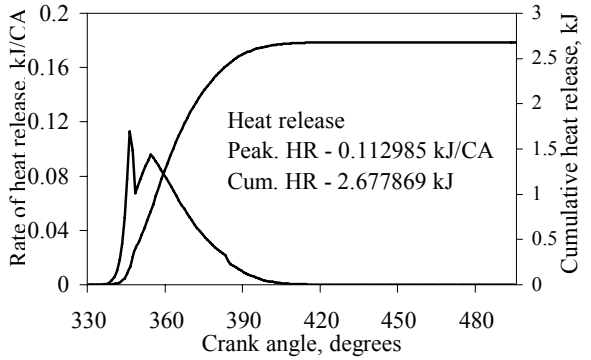

Fig. 17 Variation of heat release rate and cumulative heat release with crank angle for LHR Diesel at full load

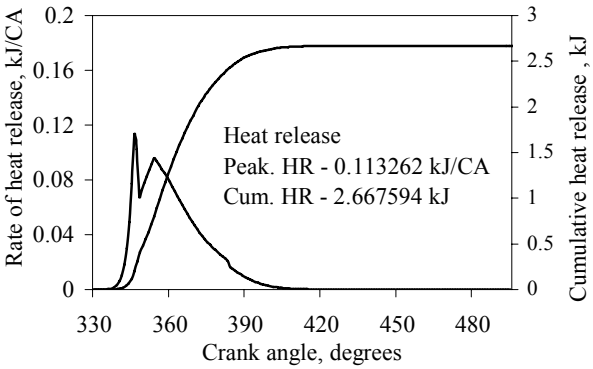

Fig. 18 Variation of heat release rate and cumulative heat release with crank angle for LHR Biodiesel at full load

Findings from the analysis are summarized as follows:

- Ignition delay period decreases for LHR engine operation and negligible reduction for biodiesel.
- Premixed burning period decreases and diffusion burning period increases.
- Total combustion duration increases for LHR operation and equally for biodiesel also.

Combustion Efficiency

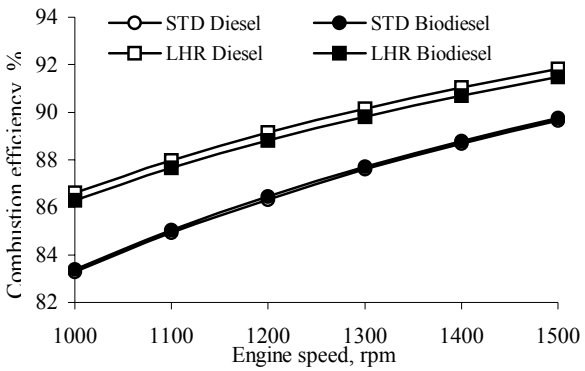

Fig. 19 Variation of combustion efficiency at full load

The combustion efficiency varies proportionately with engine speed as shown in Fig.19. Higher the combustion efficiency for LHR diesel was obtained followed by LHR biodiesel, STD biodiesel and STD diesel. Lower viscous fuel breaks in to lighter fuel particle at the end of fuel injection which increases the atomization and better combustion. In contrast higher viscous fuel increases the mixture momentum due to heavier fuel particle size. This reduction of combustion efficiency for biodiesel than diesel in LHR is due to the higher viscosity. But in contrast higher combustion efficiency was obtained for biodiesel than diesel in STD engine. The increased mixture momentum and penetration depth is responsible for this improvement.

Work Done

The variation of rate of work done and cumulative work done are shown in Fig.20 – Fig.23.

Work done for LHR diesel operation is higher due to higher peak pressure, followed by LHR biodiesel, STD biodiesel and STD diesel operation.

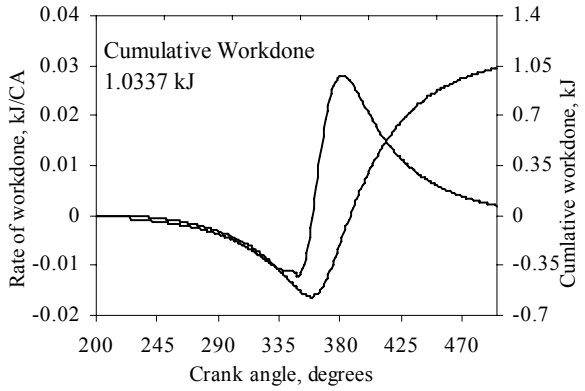

Fig. 20 Rate of work done and cumulative work done for STD diesel operation at full load

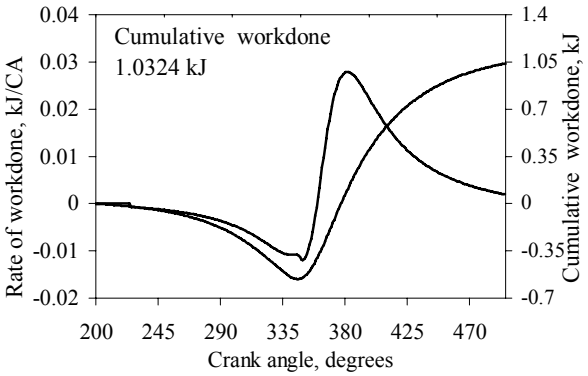

Fig. 21 Rate of work done and cumulative work done for STD biodiesel operation at full load

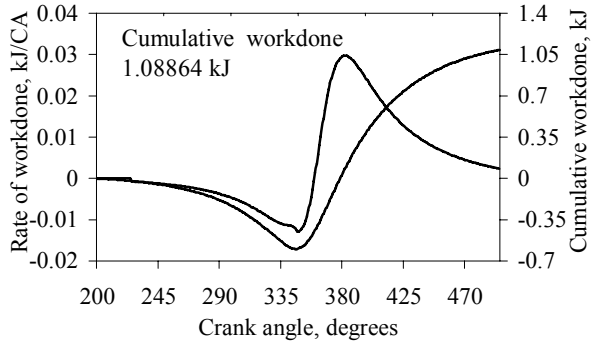

Fig. 22 Rate of work done and cumulative work done for LHR diesel operation at full load

The advantages of higher operating temperature for LHR operation are responsible for the higher work done. Higher work done leads to high thermal efficiency. Higher initial temperature of LHR operation increases the initial temperature, which reduces the volumetric efficiency. Hence higher amount of work on compression was noticed varying form 4%-5%. The energy lost during the compression process is compensated from expansion process due to increased combustion efficiency.

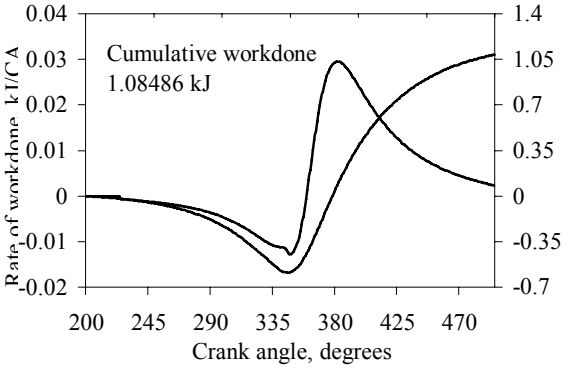

Fig. 23 Rate of work done and cumulative work done for LHR Biodiesel operation at full load

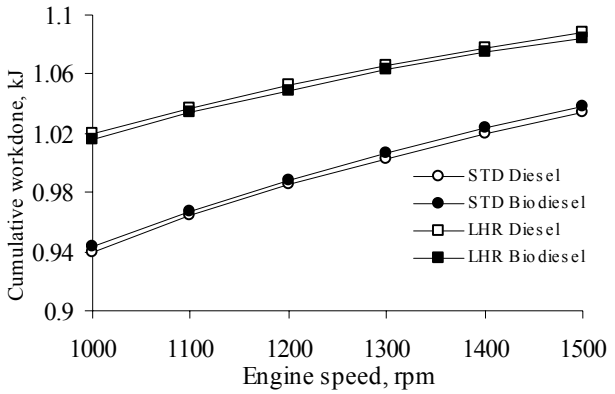

Fig. 24 Cumulative work done with engine speed at full load

Brake Thermal Efficiency

The variation of brake thermal efficiency with engine speed is shown in Fig.25. It can be seen that the brake thermal efficiency of LHR biodiesel engine is lower than that of LHR diesel and higher than STD biodiesel and STD diesel operation. However with the advantages of high operating temperature due to the presence of oxygen molecule in the biodiesel lowers the calorific value and hence the reduction in brake thermal efficiency was obtained. The calorific value of biodiesel is lower than (about 12%) that of diesel because of the presence of oxygen in its molecule. Hence, the brake thermal efficiency of LHR biodiesel is lower as compared to that of LHR diesel. The blends resulted in slightly higher efficiency than the diesel fuel, mainly due to more complete combustion [31]-[33].Lower initial temperatures and oxygenated nature of biodiesel STD operation increase the work done and hence brake thermal efficiency.

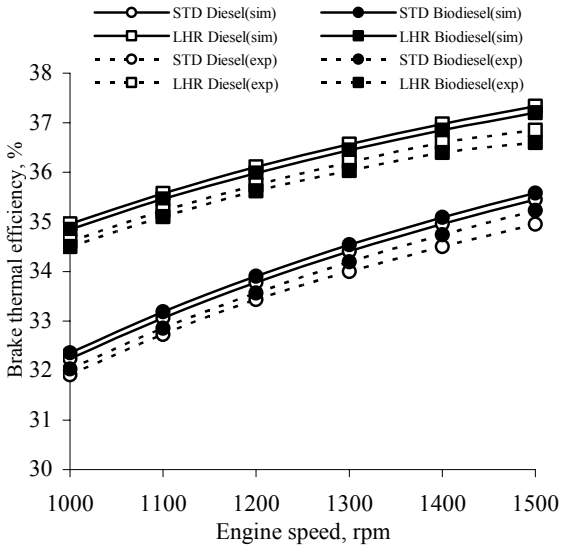

Fig. 25 Variation of brake thermal efficiency at full load

Specific Fuel Consumption

Fig.26 shows the variations of the brake specific fuel consumption (BSFC) values with respect to the engine speed. The BSFC values of the biodiesel were slightly higher than diesel fuel for STD and LHR operation. Lower the calorific value than those of the diesel fuel while they were slightly higher than those of the diesel fuel.

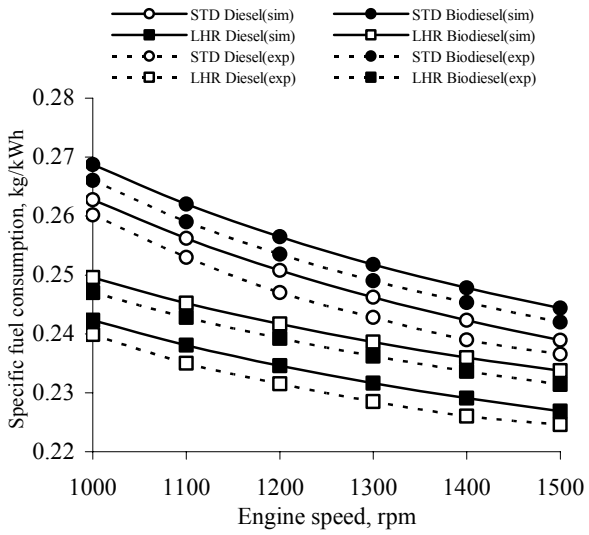

Fig. 26 Variation of specific fuel consumption at full load

VIII. CONCLUSION

A mathematical model was developed for analyzing the combustion and performance characteristics of the compression ignition engine and LHR engine. The model has been developed in such way that it can be used for characterizing any hydrocarbon fueled engines like diesel, biodiesel or their blends. The modeling results shows that, with increase in speed the peak pressure, peak temperature and brake thermal efficiency increases and decreases the specific fuel consumption. LHR engine operated with diesel shows better performance than LHR biodiesel operation but not up to the extent of lower level. However biodiesel in LHR engine shows better performance than conventional engine operation. The predicted results are compared with the experimental results of the engine fueled by diesel and B20 in STD and LHR engine. This model predicted the engine performance characteristics in closer approximation to that of experimental results. The variation in experimental and theoretical results may be due to the fact that in theoretical model homogeneous mixture with complete combustion is assumed. But in general, it is difficult to attain complete combustion. Despite the simplification resulting from the assumed hypothesis and empirical relations, the developed simulation proved to be reliable and adequate for the proposed objectives. Hence, it is believed that this mathematical model is suitable for the prediction of the combustion and

performance characteristics of the C.I engine fueled with any hydrocarbon fuel in both conventional and LHR engine.

REFERENCES

[1] Ziejewski M, Kaufman KR, "Vegetable oils as a potential alternate fuel in direct injection diesel engines", SAE Paper No. 831357, 1983.
[2] Hemmerlein N, Korte V, Richter H, Schroder G, "Performance, exhaust emissions and durability of modern diesel engines running on rapeseed oil", SAE Paper No. 910848, 1991.
[3] Ryan TW, Bagby MO, "Identification of chemical changes occurring during the transient injection of selected vegetable oils", SAE Paper No. 930933, 1993.
[4] Schlick ML, Hanna MA, Schinstock JL, "Soybean and sunflower oil performance in a diesel engine', Trans ASAE 31(5):1345–9, 1988..
[5] Dorado MP, Ballesteros E, Arnal JM, Gomez J, Lofez FJ, "Exhaust emissions from a diesel engine fueled with transesterified waste olive oil", Fuel 82:1311–5, 2003.
[6] Lang X, Dalai AK, Bakhshi NN, Reaney MJ, Hertz PB, "Preperation and characterization of bio-diesels from various bio-oils", Biosource Technol 80:53–62, 2001..
[7] Al-Widyan M, Tashtoush G, Abu-Qudais M, "Utilization of ethyl ester of waste vegetable oils as fuel in diesel engines", Fuel Process Technol 76:91–10, 2002.
[8] Monyem A, Van Gerpen JH, "The effect of biodiesel oxidation on engine performance and emissions", Biomass Bioenergy 20:317–25, 2001.
[9] Perkins LA, Peterson CL, Auld DL, "Durability testing of transesterified winter rape oil as fuel in small bore, multi-cylinder, DI, CI engines", SAE Paper No. 911764, 1991.
[10] Zhang Q, FeldmanM, Peterson CL, "Diesel engine durability when fueled with methyl ester of winter rapeseed oil", ASAE paper No. 881562, 1988.
[11] Abderrahim Bouaid, Mercedes Martinez, Jose Aracil, "A comparative study of the production of ethyl esters from vegetable oils as a biodiesel fuel optimization by factorial design", Chemical Engineering Journal 134 ,93–99, 2007.
[12] A.S. Ramadhas, S. Jayaraj, C. Muraleedhara, "Biodiesel production from high FFA rubber seed oil", Fuel 84 335–340, 2005.
[13] Ayhan Demirba, "Comparison of transesterification methods for production of biodiesel from vegetable oils and fats", Energy Conversion and Management 49 125–13, 2008.
[14] L.C. Meher a, Vidya S.S. Dharmagadda b, S.N. Naik, "Optimization of alkali-catalyzed transesterification of *Pongamia pinnata* oil for production of biodiesel", Bioresource Technology 1392–1397, 97, 2006.
[15] Sanjib Kumar Karmee, Anju Chadha, "Preparation of biodiesel from crude oil of Pongamia pinnat", Bioresource Technology 96, 1425–1429, 2005.
[16] James A. Leidel, "An Optimized Low Heat Rejection Engine for Automotive Use - An Inceptive Study", SAE Paper No. 970068, 1997.
[17] Abdullah Uzun a,*, I˙smet C¸ evik b, Mustafa Akc¸il, "Effects of thermal barrier coating on a turbocharged diesel engine performance", Surface and Coatings Technology 116–119, 505–507, 1999.
[18] Ekrem Bu¨yu¨kkaya *, Tahsin Engin, Muhammet Cerit, "Effects of thermal barrier coating on gas emissions and performance of a LHR engine with different injection timings and valve adjustments", Energy Conversion and Management 47, 1298–1310, 2006.
[19] I. TaymazT, K. C¸ akVr, A. Mimaroglu, "Experimental study of effective efficiency in a ceramic coated diesel engine", Surface and Coatings Technology 200, 1182– 1185, 2005.
[20] S.Jaichandar and P.Tamilporai, "Low Heat Rejection Engines – An Overview", SAE 2003-01-0405,2003.
[21] Imdat Taymaz, "The effect of thermal barrier coatings on diesel engine performance", Surface and Coatings Technology 201, 5249–5252, 2007.
[22] P.Tamilporai," Simulation and analysis of combustion and heat transfer in low heat rejection diesel engine using two zone combustion model and different heat transfer models" PhD thesis, Anna University, India.1998.
[23] B.Rajendra Prasath, P.Tamilporai, Mohd.F.Shabir, "Simulation and Analysis of Combustion, Performance and Emission Characteristics of Biodiesel Fueled Low Heat Rejection Direct Injection Diesel Engine", SAE Paper No. 2007-32-0094.
[24] Jonh. B. Heywood, "Internal combustion engines fundamentals", Tata McGraw Hill book company; 1989.
[25] Ganesan V, "Computer simulation of compression ignition engines", University Press (India) Ltd.; 2000.
[26] P.Tamilporai, N.Baluswamy, " Simulation and analysis of heat transfer in low heat rejection direct injection diesel engines using a two zone model" 3 rd Asian – Pacific international symposium on Combustion and energy utilization.1998.
[27] Fangrui Maa, Milford A. Hannab," Biodiesel production: a review" Bioresource Technology 70, 1-15, 1999.
[28] P. Chitra, P. Venkatachalam and A. Sampathrajan, "Optimisation of experimental conditions for biodiesel production from alkali-catalysed transesterification of Jatropha curcus oil" Article from Department of Bio-Energy, AEC & RI, TamilNadu Agricultural University, Coimbatore-641 003, Tamil Nadu, India, 2005.
[29] A.S. Ramadhas_, S. Jayaraj, C. Muraleedharan, "Theoretical modeling and experimental studies on biodiesel-fueled engine", Renewable Energy 31, 1813–1826. 2006.
[30] Rakopoulos CD, Hountalas DT, Zannis TC, "Theoretical study concerning the effect of oxygenated fuels on DI Diesel engine performance and emissions" SAE Paper No. 2004-01-1838, 2004.
[31] Rakopoulos , K.A. Antonopoulos, D.C. Rakopoulos," Development and application of multi-zone model for combustion and pollutants formation in direct injection diesel engine running with vegetable oil or its bio-diesel", Energy Conversion and Management 48, 1881–1901, 2007.
[32] Gonzalez Gomez ME, Howard-Hildige R, Leahy JJ, O_Reilly T, Supple B, Malone M, "Emission and performance characteristics of a 2 litre Toyota Diesel van operating on esterified waste cooking oil and mineral diesel fuel", Environ Monit Assess 65,13–20, 2000.
[33] Pramanik K, " Properties and use of jatropha curcas oil and diesel fuel blends in compression ignition engine. Renew Energy 28(2):239–48, 2003.
[34] Al-Widyan MI, Tashtoush G, Abu-Qudais M, " Utilization of ethyl ester of waste vegetable oils as fuel in diesel engines", Fuel Process Technol 76,91–103, 2000..